Higher smectic-layer order parameters in liquid crystals determined by x-ray diffraction and the effect of antiferroelectricity

Yoichi Takanishi, Asako Ikeda, Hideo Takezoe, and Atsuo Fukuda
Department of Organic and Polymeric Materials, Tokyo Institute of Technology, O-okayama, Meguro-ku, Tokyo 152, Japan
(Received 15 June 1994)

By observing the higher-order Bragg peaks corresponding to the layer spacing, the smectic-layer order parameters up to the third order were obtained and the center-of-mass distribution function along the layer normal was calculated. The results clearly indicate that the smectic layer distribution is different from a sinusoidal density wave in antiferroelectric liquid crystals and that the smectic- (Sm) layer order is relatively higher in antiferroelectric Sm-$C_A^{(*)}$ than in ferroelectric Sm-$C^{(*)}$. There exists a correlation between the stable antiferroelectricity and the higher smectic-layer order.

PACS number(s): 61.30.Eb, 77.80.−e, 61.10.−i

I. INTRODUCTION

The intermolecular interactions stabilizing the (chiral) nematic ($N^{(*)}$) and smectic-A (Sm-A) phases are reasonably well understood. Although the situation in the (chiral) smectic-C (Sm-$C^{(*)}$) phase is less clear, a number of microscopic models for the Sm-$C^{(*)}$ phase that display the Sm-A–Sm-$C^{(*)}$ phase transition have been devised so far. All of them took it for granted that molecules tilt in the same direction and sense in subsequent layers, probably due to a notion that the smectic layer is very close to a sinusoidal density wave and that the usual picture of molecules lying on equidistant planes is far from correct. Actually, in Sm-A, Als-Nielsen *et al.* [1] and Stamatoff *et al.* [2] found that the second-order peak in x-ray diffraction was either absent or, when it did occur, down three or four orders of magnitude in intensity from the first-order one. By combining this density wave character of the layer with Meyer's mechanism [3] for the emergence of spontaneous polarization, we can infer that the packing entropy due to the excluded volume effect stabilizes ferroelectricity in chiral smectic liquid crystals.

In 1989, Chandani *et al.* [4] and Fukada *et al.* [5] found antiferroelectricity in MHPOBC (see below), noticing that tristable switching is the electric-field-induced phase transition between antiferroelectric chiral smectic-C_A (Sm-C_A^*) and ferroelectric Sm-C^*. They proposed that Sm-C_A^* has a herringbone structure in which molecules tilt in the same direction but opposite senses in adjacent smectic layers aside from slight precession in the tilting direction from layer to layer. Its appropriateness was confirmed in the visible-light wavelength scale by observing the characteristic Bragg reflection of light due to the helicoidal structure. Beresnev *et al.* [6] and Galerne and Liebert [7] also proposed an antiferroelectric herringbone structure, but did not confirm that a strong enough electric field induces a transition from the antiferroelectric Sm-C_A^* structure to the ferroelectric Sm-C^* structure. An important open question was: What is the intermolecular interaction stabilizing antiferroelectric Sm-C_A^*? Takanishi *et al.* [8] proposed the pair formation of transverse dipole moments in adjacent smectic layers as the cause of the antiferroelectricity. This proposal implies that the interlayer packing of molecules may become tighter. Actually, Ikeda *et al.* [9] reported that the compounds with the stable antiferroelectric phase have thinner layer thickness than those with a stable ferroelectric phase.

The sinusoidal density wave character of the smectic layer may be incompatible with the antiferroelectric Sm-C_A^* structure; it could not be decided in which of the two possible senses the molecules may tilt in the minimum density region. In this paper, we report the degree of the smectic-layer order in the ferroelectric Sm-C^* and antiferroelectric Sm-C_A^* phases studied by x-ray diffraction. We measured the first- and higher-order Bragg peaks corresponding to the layer thickness. From the integrated peak intensities, we calculated the smectic-layer order parameters and the Gaussian distribution function of mass density of molecules along the layer normal. The smectic-layer order in Sm-C is first compared with that in Sm-C_A in a racemic compound. The comparison is then made between the smectic-layer order parameters in Sm-C^* and Sm-C_A^* in two different compounds which have similar chemical structures but different phase sequences. We found that the smectic-layer order in the Sm-$C_A^{(*)}$ phase is relatively higher than that in the Sm-$C^{(*)}$ phase, as expected. Although intense higher harmonics have already been observed in polar and/or polymeric liquid crystals [10–12], only a few investigations [13,14], specifically none in antiferroelectric liquid crystals, have been made from a standpoint of obtaining the smectic-layer order parameters.

II. EXPERIMENT

Compounds used were a racemic MHPOBC, (R)-10BIMF6, and (R)-10BIMF7 [9], whose chemical struc-

TABLE I. Chemical structures and phase sequences of materials used.

MHPOBC(racemate)	$C_6H_{17}O$-Ph-Ph-COO-Ph-COO-CH(CH_3)C_6H_{13}
	iso $\xrightarrow{140\,^\circ C}$ Sm-A $\xrightarrow{120\,^\circ C}$ Sm-C $\xrightarrow{113\,^\circ C}$ Sm-C_A
10BIMF6	$C_{10}H_{21}O$-Ph-Ph-COO-(F)Ph-COO-$\overset{*}{C}$H(CF_3)C_6H_{13}
	iso $\xrightarrow{95.0\,^\circ C}$ Sm-A $\xrightarrow{76.9\,^\circ C}$ Sm-C^*_A $\xrightarrow{30\,^\circ C}$ Cryst
10BIMF7	$C_{10}H_{21}O$-Ph-Ph-COO-(F)Ph-COO-$\overset{*}{C}$H(CF_3)C_7H_{15}
	iso $\xrightarrow{88.3\,^\circ C}$ Sm-A $\xrightarrow{70.2\,^\circ C}$ Sm-C^* $\xrightarrow{30\,^\circ C}$ Cryst

tures and phase sequences are presented in Table I. The compound dropped on a cover glass was extended to be thin during heating up to the isotropic–Sm-A transition point, and gradually cooled down [9]. These sample cells were well homeotropically aligned as confirmed by x-ray diffraction, as shown in Fig. 1(a), and by optical microscope observation. The film thickness was about 25 μm.

We used a Rigaku RU-200 x-ray system (Ni-filtered Cu $K\alpha$ line, 12 kW) equipped with a temperature control unit (within $\pm 0.1\,^\circ$C accuracy) [15]. To obtain the accurate value of the layer thickness, the diffraction angle was calibrated by using the lattice constants of stearic acid measured in the same condition. This calibration assures the accuracy of ± 0.1 Å in the absolute layer thickness. The first- and higher-order Bragg peaks corresponding to the layer thickness were measured by the conventional $2\theta-\theta$ method. The multiple scattering effect on the higher-order peaks is reported by Stamatoff *et al.* [2] and Ocko *et al.* [16]. According to their papers, the second-order harmonic peak from the primary beam is detected at $q=2q_0$ and $\omega=2\theta_0$, when a fundamental first-order one is observed at $q=q_0$ and $\omega=\theta_0$, while multiple scattering peaks appear at $q=2q_0$, $\omega=\theta_0$, and $3\theta_0$. This effect investigated following their method indicates that the higher-order peaks detected come from the primary x-ray beam, as shown in Fig. 1(b).

In order to detect higher-order peaks that are considerably smaller than the first-order peak, stronger x-ray power is preferable so long as the counts/s at the first-order peak does not saturate a scintillation counter. To make sure of the linearity, Fig. 2 was obtained by measuring the first- and second-order Bragg peaks corresponding to the layer thickness in the Sm-A phase of octyl cyanobiphenyl (8CB); the ratio of the second-order integrated peak intensity to the first-order one, I_2/I_1, is 4.4×10^{-4}, almost the same as Stamatoff *et al.*'s data (3.8×10^{-4}) [2]. Typical peak profiles of first, second, and third orders in MHPOBC are shown in Fig. 3. In evaluating the integrated peak intensities, we took account of the Lorentz polarization factor but not the temperature factor.

III. RESULTS

Figure 4(a) shows the temperature dependence of the layer spacing, d, in racemic MHPOBC. The layer spacing is almost constant in Sm-A and monotonically decreases from the Sm-A–Sm-C phase transition point on

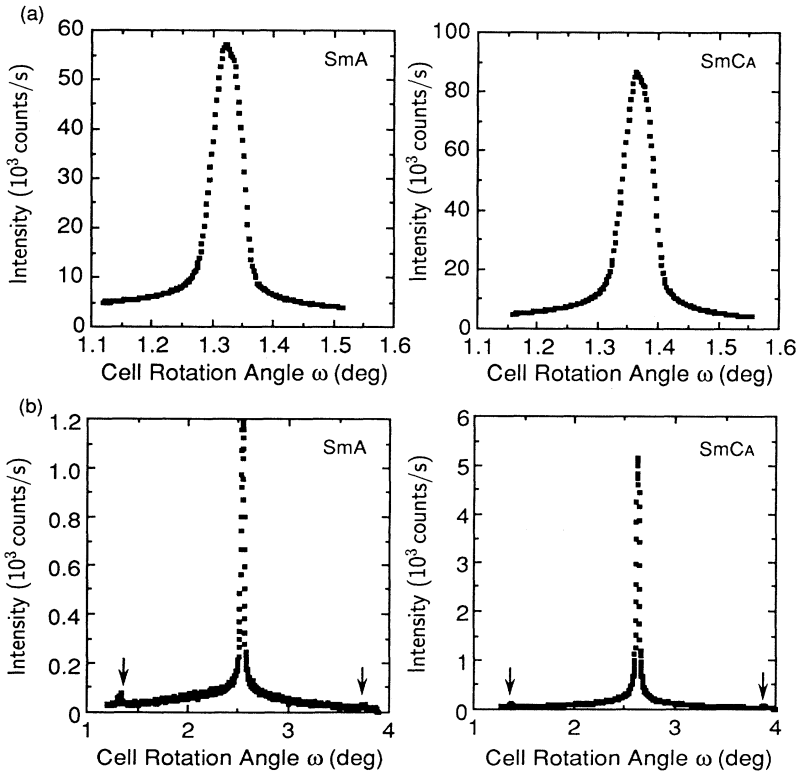

FIG. 1. (a) Intensity curve profiles against the cell rotation angle ω in the Sm-A and Sm-C_A phases. The half width of the peak is about 0.05°, showing that the smectic layer is well oriented parallel to the glass substrate in the droplet sample. (b) Rocking curve profiles at $(0,0,2\theta_0)$ in the Sm-A and Sm-C_A phases. The central peak corresponds to the second-order harmonic peak, and the others to the multiple scattering.

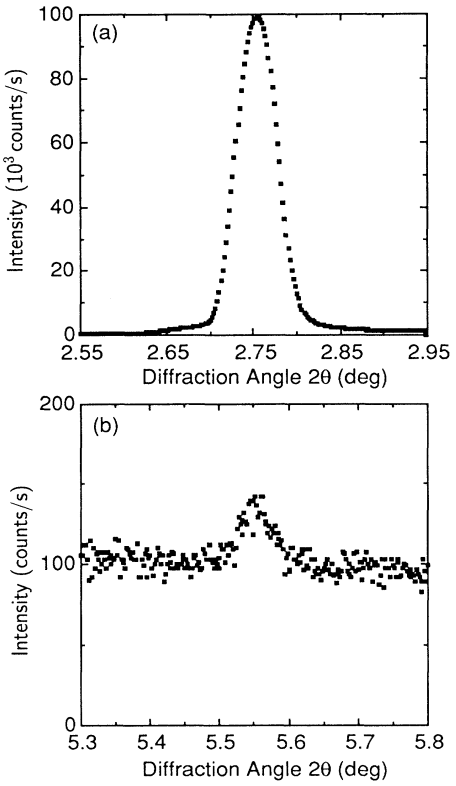

FIG. 2. Intensity curve profiles of the (a) first- and (b) second-order peaks corresponding to the layer thickness of 8CB. The third-order peak could not be observed.

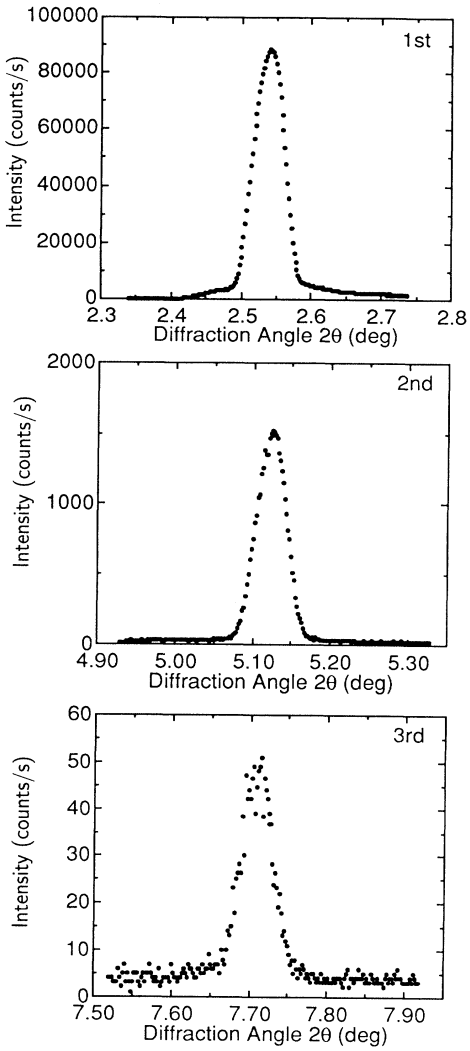

FIG. 3. Intensity curve profiles of the first-, second-, and third-order peaks corresponding to the layer thickness of MHPOBC at $T=90\,^{\circ}\mathrm{C}$ (Sm-C_A).

cooling. It jumps slightly at the Sm-C–Sm-C_A phase transition point, indicating the first-order character of the phase transition. The layer thickness jump has already been reported in TFMHPOBC by Yamawaki *et al.* [17]. Figures 4(b)–4(d) show the temperature dependence of the first-, second-, and third-order integrated peak intensities. The first- and second-order ones attain their minima in the vicinity of the Sm-A–Sm-C phase transition point, where the layer rearrangement begins to occur because of the molecular tilting from the layer normal. With decreasing temperature, both the intensities increase again below this temperature and even the third-order one appears in Sm-C and Sm-C_A. All integrated intensities rise discontinuously at the Sm-C–Sm-C_A phase transition point. The first-order one saturates at lower temperatures in Sm-C_A, while the second- and third-order ones increase monotonically without showing any saturation.

Figure 5(a) is the temperature dependence of the layer spacing in 10BIMF6 and 10BIMF7, where the Sm-A–Sm-C_A^* and Sm-A–Sm-C^* phase transition temperatures are indicated by T_c. The layer spacing changes almost similarly in the two materials; the layer is much thinner in 10BIMF6 (Sm-C_A^*) than in 10BIMF7 (Sm-C^*) as already discussed in detail by Ikeda *et al.* [9]. Figures 5(b)–5(d) are the temperature dependence of the first-, second-, and third-order integrated peak intensities. The third-order peak is observed even in Sm-A, and all the intensities in Sm-C_A^* are much stronger than those in Sm-C^*, although the 10BIMF6 molecule has less electrons than the 10 BIMF7 one. Even in the Sm-A phase, the higher-order-peak integrated intensity is stronger in 10BIMF6 showing Sm-C_A^* than in 10BIMF7 showing Sm-C^*, while this tendency is less clear in the first-order-peak integrated intensities.

Temperature may influence the intensity; in general, an x-ray-diffraction peak at higher temperatures is smaller than that at lower ones because of the lattice vibration. In the present case, however, the Sm-A–Sm-C_A^* transition temperature in 10BIMF6 is higher than the Sm-A–Sm-C^* transition temperature in 10BIMF7. Thus the intensity differences between Sm-C_A^* and Sm-C^* cannot be ascribed to the temperature factor.

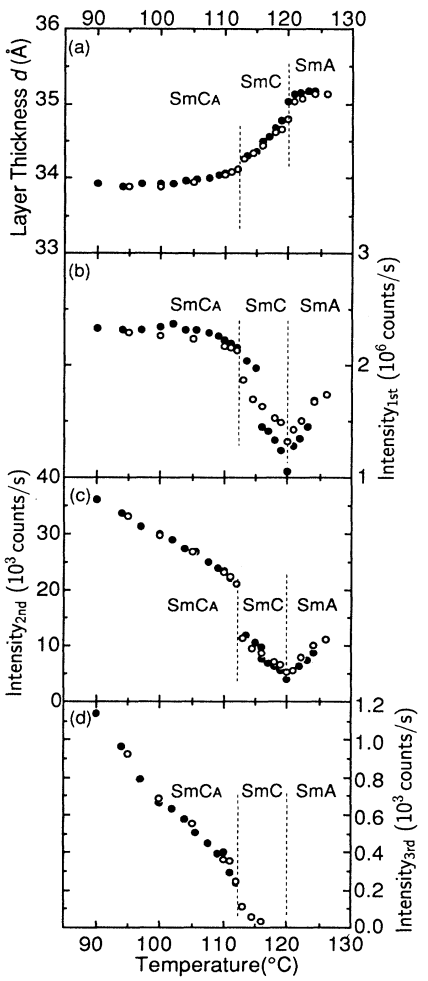

FIG. 4. Temperature dependence of (a) the layer spacing and (b)–(d) the integrated peak intensities of the first, second, and third order in racemic MHPOBC. Open and closed circles are for the heating and cooling processes, respectively. Some discontinuity is observed at the Sm-C–Sm-C_A phase transition.

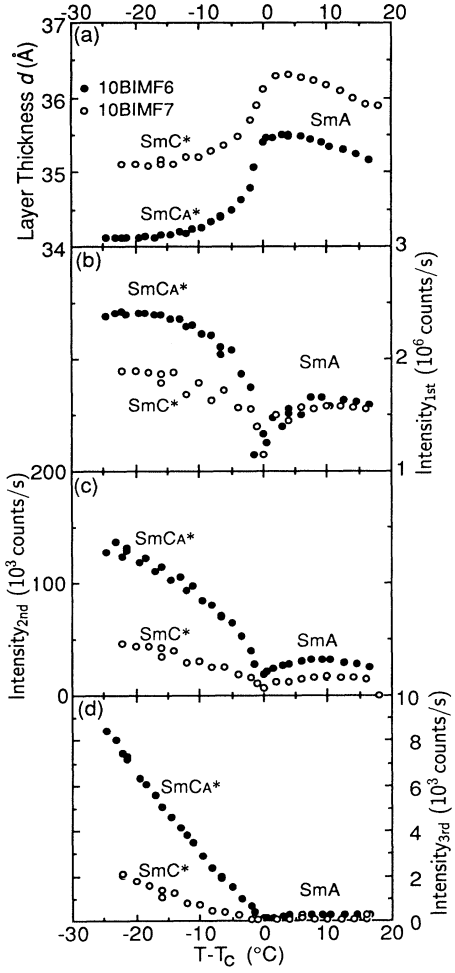

FIG. 5. Temperature dependence of (a) the layer spacing, and (b) first-, (c) second-, and (d) third-order integrated peak intensities in 10BIMF6 (closed circles) and 10BIMF7 (open circles).

IV. DISCUSSION

Using the ratios among the integrated intensities of the first-, second-, and third-order diffraction peaks, we calculated the smectic-layer order parameters without taking account of the smectic-layer undulation. According to the McMillan theory [18], the distribution function of the molecular center of gravity along the layer normal, $f(z)$, is expanded into

$$f(z)=\frac{1}{d}\left[1+\sum_{l=1}^{\infty}2\tau_l\cos\left[\frac{2\pi l}{d}z\right]\right], \tag{1}$$

where the coordinate z is parallel to the layer normal, and τ_l is the lth smectic-layer order parameter,

$$\tau_l=\left\langle\cos\left[\frac{2\pi l}{d}z\right]\right\rangle=\int_0^d f(z)\cos\left[\frac{2\pi l}{d}z\right]dz\ . \tag{2}$$

When $\tau_l=1$ for any l, the layer is formed perfectly, as in a crystal where molecules lie on equidistant planes; when $\tau_l=0$, on the other hand, the layer does not exist as in the nematic phase. The lth-order integrated peak intensity is given by

$$I(00l)=C\tau_l^2|F(00l)|^2\quad(C:\ \text{const})\ , \tag{3}$$

where $F(00l)$ is the molecular structure factor calculated by using the molecular shape model with the minimum steric energy. Numerically obtained $|F(002)|^2/|F(001)|^2$ and $|F(003)|^2/|F(001)|^2$ are listed in Table II. Watanabe and Hayashi [19] reported that $F(00l)$ is not sensitive to the fine details of the molecular shape, and we also confirmed it. We assumed that molecules do not change the conformation seriously through the transition from Sm-A to Sm-$C^*_{(A)}$, because d varies with temperature so normally that it is proportional to the cosine of the molecular apparent tilt angle. Substituting the experi-

TABLE II. Numerically calculated ratios $|F(002)|^2/|F(001)|^2$ and $|F(003)|^2/|F(001)|^2$.

	MHPOBC	10BIMF6	10BIMF7
$\|F(002)\|^2/\|F(001)\|^2$	0.1460	0.1577	0.0872
$\|F(003)\|^2/\|F(001)\|^2$	0.0261	0.0277	0.0894

mental results of $I(002)/I(001)$ and $I(003)/I(001)$ and the calculated results of $F(001)$, $F(002)$, and $F(003)$ into Eq. (3), we can determine τ_2/τ_1 and τ_3/τ_1.

It is necessary for further discussion to assume the distribution function as an appropriate form. We supposed it to be Gaussian according to Leadbetter and Norris's paper [20],

$$f(z)=\frac{1}{\sqrt{2\pi\langle z^2\rangle}}\exp\left[-\frac{z^2}{2\langle z^2\rangle}\right]. \tag{4}$$

Here $\langle z^2\rangle^{1/2}$ is the rms of the displacement of the molecules along the layer normal. We obtain τ_l ($l=1$, 2, and 3) by solving Eqs. (1) and (4) using the Laplace integral

$$\tau_l=\exp\left[-\frac{2\pi^2 l^2\langle z^2\rangle}{d^2}\right]. \tag{5}$$

By transforming Eq. (5), we can obtain $\langle z^2\rangle$ as follows:

$$\langle z^2\rangle=-\frac{d^2}{2\pi^2 l^2}\ln|\tau_l|\ . \tag{6}$$

Equation (5) further gives the relation between τ_l and τ_1,

$$\tau_l=\tau_1^{l^2}\ . \tag{7}$$

Therefore, from Eq. (7) and τ_l/τ_1 determined by Eq. (3), we can obtain τ_l independently.

Figure 6(a) shows the temperature dependence of the smectic-layer order parameters in racemic MHPOBC thus obtained. τ_1 determined from τ_2/τ_1 is almost the same as that determined from τ_3/τ_1, indicating that the assumption of the Gaussian distribution is reasonable. All τ_l's increase discontinuously at the Sm-C–Sm-C_A phase transition. Figures 6(b) and 6(c) show the temperature dependence of τ_l ($l=1$, 2, and 3) in 10BIMF6 and 10BIMF7, respectively. All τ_l's increase monotonically with decreasing temperature in Sm-C^* and Sm-C_A^*. In Sm-C_A^* of 10BIMF6, τ_1 attains 0.9, and τ_2 and τ_3 are larger than those in Sm-C^* of 10BIMF7. Even in Sm-A, all parameters of 10BIMF6 are larger than those of 10BIMF7. This fact is consistent with the results that the stability of antiferroelectricity affects the smectic-layer spacing even in Sm-A, as reported by Ikeda *et al.* [9].

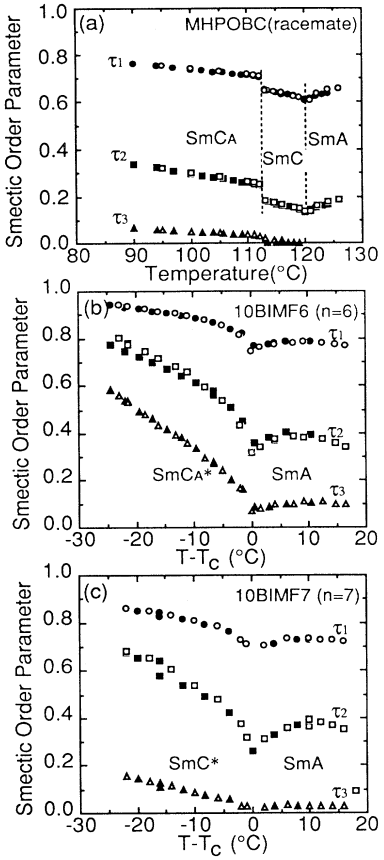

FIG. 6. Temperature dependence of the smectic order parameters τ_1, τ_2, and τ_3 in (a) racemic MHPOBC, (b) 10BIMF6 and (c) 10BIMF7. A discontinuous jump is observed at the Sm-C–Sm-C_A phase transition in MHPOBC. The open and closed symbols are for the heating and cooling processes, respectively.

Substituting the above results into Eqs. (4) and (6), we can obtain the mass density distribution along the layer normal, $f(z)$, in the Sm-A, Sm-$C^{(*)}$, and Sm-C_A phases of the three compounds, as illustrated in Fig. 7. A dotted line indicates a simple sinusoidal wave corresponding to the case of $\tau_1=0.5$ and $\tau_l=0$ ($l=2,3\ldots$). It is clearly seen that the actual profiles are far different from the sinusoidal curve even in Sm-A, although the profile of 8CB almost coincides with the sinusoidal curve [2]. In MHPOBC, it is noted that the profiles in Sm-A and Sm-C are almost the same, although the measurement temperatures for the profiles are very different ($\Delta T=11$ °C). At the phase transition from Sm-C to Sm-C_A, however, the profile abruptly changes, becoming considerably sharper. With decreasing temperature, the profile grows sharper in Sm-C_A. Similarly, a comparison between 10BIMF6 and 10BIMF7 reveals that the smectic layer in Sm-C_A^* is more highly ordered than that in Sm-C^*. However, the narrower standard deviation, i.e., the higher smectic-layer order, does not always mean the emergence of Sm-C_A^*, as is clear by comparing racemic MHPOBC and

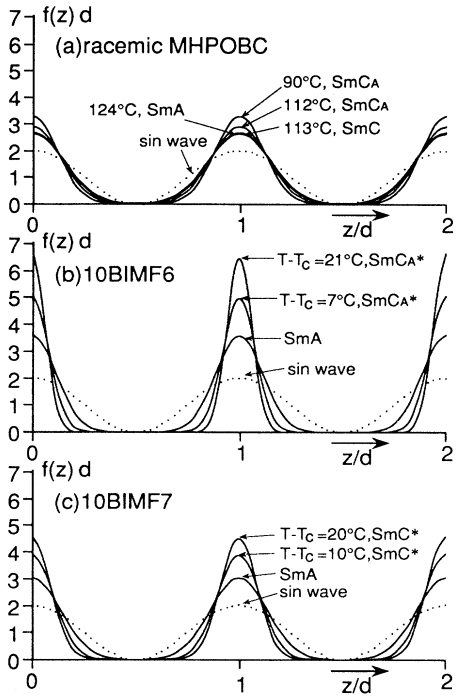

FIG. 7. The normalized distribution function of the mass density along the layer normal, $f(z)d$, at various temperatures in (a) racemic MHPOBC, (b) 10BIMF6, and (c) 10BIMF7. A dotted line shows the sinusoidal curve with $\tau_1=0.5$.

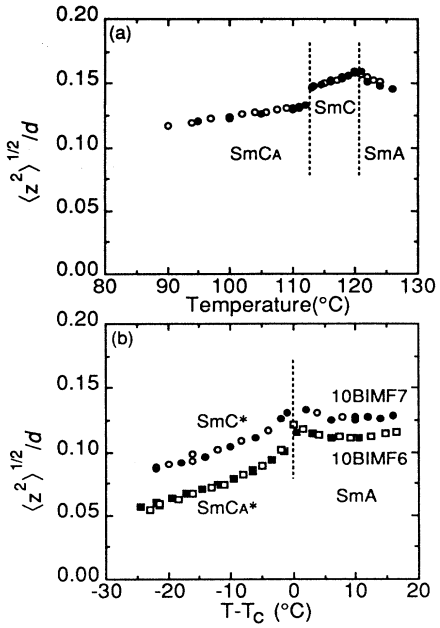

FIG. 8. Temperature dependence of the standard deviation $\langle z^2\rangle^{1/2}/d$ in (a) racemic MHPOBC and (b) 10BIMF6 and 10BIMF7. The open and closed symbols are for the heating and cooling processes, respectively.

10BIMF7. Therefore, the higher smectic-layer order is the necessary but not sufficient condition for the antiferroelectricity. The standard deviation $\langle z^2\rangle^{1/2}/d$ is summarized in Fig. 8.

V. CONCLUSION

In this way, it is well established that the center-of-mass distribution along the smectic-layer normal is sometimes quite different from a sinusoidal wave but is consistent with a Gaussian function even when the smectic layer is two dimensional liquidlike. Moreover, there is a tendency for the standard deviation to be narrower; in other words, the smectic-layer order is relatively higher in Sm-C_A^* than in Sm-C^* when it is possible for a comparison to be made in a particular substance where both phases emerge, or in a homologous series of substances where the odd-even effect of the Sm-C_A^* emergence is observed, although the absolute smectic-layer order alone does not determine the Sm-$C_A^{(*)}$ emergence. We insist that not only the Sm-$C_A^{(*)}$ but also the Sm-A and Sm-$C^{(*)}$ layers are not always simple sinusoidal density waves, and one must be cautious in discussing the smectic elasticity and the molecular interactions between neighboring layers.

ACKNOWLEDGMENTS

This work was partly supported by a Grant-in-Aid for Scientific Research (Specially Promoted Research No. 06102005) from the Ministry of Education, Science and Culture. We acknowledge Kashima Oil Co., Ltd. for supplying 10BIMF6 and 10BIMF7.

[1] J. Als-Nielsen, R. J. Birgeneau, M. Kaplan, J. D. Listster, and C. R. Safinya, Phys. Rev. Lett. **39**, 352 (1977); **39**, 1668 (1977).
[2] J. Stamatoff, P. E. Cladis, D. Guillon, M. C. Cross, T. Bilash, and P. Finn, Phys. Rev. Lett. **44**, 1509 (1980).
[3] R. B. Meyer, L. Liebert, L. Strzelecki, and P. Keller, J. Phys. (Paris) **36**, L69 (1975).
[4] A. D. L. Chandani, E. Gorecka, Y. Ouchi, H. Takezoe, and A. Fukuda, Jpn. J. Appl. Phys. **28**, L1265 (1989).
[5] A. Fukuda, Y. Takanishi, T. Isozaki, K. Ishikawa, and H. Takezoe, J. Mater. Chem. **4**, 997 (1994).
[6] L. A. Beresnev, L. M. Brinov, M. A. Osipov, and S. A. Pikin, Mol. Cryst. Liq. Cryst. **158A**, 3 (1988).
[7] Y. Galerne and L. Liebert, Phys. Rev. Lett. **66**, 2891 (1991).
[8] Y. Takanishi, K. Hiraoka, V. K. Agrawal, H. Takezoe, A. Fukuda, and M. Matsushita, Jpn. J. Appl. Phys. **30**, 2023 (1991).
[9] A. Ikeda, Y. Takanishi, H. Takezoe, and A. Fukuda, Jpn. J. Appl. Phys. **32**, L97 (1993).
[10] P. Davidson and A. M. Levelut, Liq. Cryst. **11**, 469 (1992).
[11] P. Davidson and L. Strzelecki, Liq. Cryst. **3**, 1583 (1988).
[12] E. Nachaliel, E. N. Keller, D. Davidov, and C. Boeffel, Phys. Rev. A **43**, 2897 (1991).
[13] R. M. Richardson and N. J. Herring, Mol. Cryst. Liq. Cryst. **123**, 143 (1985).

[14] E. F. Gramsbergen and W. H. De Jeu, Liq. Cryst. **4**, 449 (1989).

[15] Y. Ouchi, J. Lee, H. Takezoe, A. Fukuda, K. Kondo, T. Kitamura, and A. Mukoh, Jpn. J. Appl. Phys. **27**, L725 (1988).

[16] B. M. Ocko, A. R. Kortan, R. J. Birgeneau, and J. W. Goodby, J. Phys. (Paris) **45**, 113 (1984).

[17] M. Yamawaki, Y. Yamada, N. Yamamoto, K. Mori, H. Hayashi, Y. Suzuki, Y. S. Negi, T. Hagiwara, I. Kawamura, H. Orihara, and Y. Ishibashi, in *Proceedings of the Ninth International Display Research Conference, Japan Display '89, Kyoto 1989,* edited by A. Sasaki, T. Kojima, and H. Uchiike (Society for Information Display, Playa del Rey, California and The Institute of Television Engineers of Japan, Tokyo, 1989), p. 26.

[18] W. L. McMillan, Phys. Rev. A **6**, 936 (1972).

[19] J. Watanabe and M. Hayashi, Macromolecules **22**, 4083 (1989).

[20] A. J. Leadbetter and E. K. Norris, Mol. Phys. **38**, 669 (1979).